Probabilistic Reliability Assessment of Real-Time Hybrid Simulation of Structures with Degradation

Hezareigh Ryan
Graduate Student, School of Engineering, San Francisco State Univ., San Francisco, USA

Cheng Chen
Assistant Professor, School of Engineering, San Francisco State Univ., San Francisco, USA

Samuel Richardson
Graduate Student, School of Engineering, San Francisco State Univ., San Francisco, USA

ABSTRACT: Improving seismic performance of structures and seismic design codes requires that laboratory experiments truthfully replicate the seismic structural response. Real-time hybrid simulation provides a viable alternative for shake table testing that allows more economical and efficient seismic performance evaluation in size-limited laboratories. Not well-understood critical parts of the structure are tested physically as experimental substructures in the laboratory, while well-behaved parts are numerically modeled by computer programs as analytical substructures. Servo-hydraulic actuators impose desired responses onto the experimental substructures. Restoring forces from substructures are integrated by a numerical algorithm to enable the replication of the entire structural response through large- or full-scale component tests. However, actuator delay causes a deviation from the exact structural response. This creates a great challenge for reliability assessment of real-time hybrid simulation results since the actual structural response is not available before or after the experiment for an immediate comparison. This paper presents a probabilistic reliability assessment approach for real-time hybrid simulation of structures with degradation. With the generalized Bouc-Wen model to emulate strength and stiffness degradation of structures close to collapse, computational simulation are conducted on single-degree-of-freedom structures subjected to selected ground motions with different intensities. Different natural frequencies are considered as well as slight, moderate and significant degradation. A lognormal distribution for critical delay corresponding to target accuracy is then established to enable probabilistic reliability assessment without actual response known a priori. Examples of applying the proposed probabilistic approach are also presented in this paper.

1. INTRODUCTION

Earthquakes pose a threat to structures, their content, and their occupants. Although human death and injury are of highest concern, earthquakes can result in significant economic loss. Improving seismic structural performance thus is of great significance for earthquake engineering community. This cannot be achieved without seismic structural testing which could be prohibitively expensive. The most widely used methods include quasi-static testing and shake table testing. The former is a more economical option, while the latter, though much more expensive, is more suitable for evaluating seismic structural response, especially when testing with rate-dependent components such as dampers. Another more recent approach is real-time hybrid simulation (RTHS) which provides a much more viable alternative for shake table testing. RTHS takes advantage of the knowledge available on the behavior of well-understood members and components by substructuring them from the prototype structure and modeling them analytically. The rest of the structure, the new, more complex, and not well-known components, are experimentally tested in the laboratory. Equilibrium and compatibility conditions are imposed at the boundaries between the analytical and experimental substructures (Chen *et al.* 2009). Servo-hydraulic actuators then impose desired responses onto the experimental substructures. The resulting restoring forces are measured and fed back to an integration algorithm to calculate the structural response for the following time steps. RTHS thus not only allows testing of rate dependent components, it also costs significantly less than shake table tests of similar scales.

The actuators used in RTHS have intrinsic delay to the displacement command due to servo-hydraulic dynamics. This delay, even though in millisecond (ms) magnitude, could significantly affect the experimental results from real-time hybrid simulation. Figure 1 presents the discrepancy for a single-degree-of-freedom (SDOF) structure between the true (exact) response and the response from real-time hybrid simulation with two milliseconds delay in actuator response. A maximum difference of 45.5 mm can be observed corresponding to 54.1% of maximum displacement of exact response. It is therefore necessary to have actuator delay compensation to achieve reliable RTHS results. However, experimental studies have indicated that even the most sophisticated compensation method cannot completely eliminate actuator delay induced tracking error (Chen 2010, Chen *et al.* 2012). It is therefore important to perform reliability assessment of RTHS results, especially when the actual structural response is not known a priori for comparison. Chen and Sharma (2012) studied the accuracy of RTHS for SDOF structures and proposed a probabilistic approach for reliability assessment of RTHS results with presence of actuator delay. Chen *et al.* (2013) further investigated the effect of nonlinearity and improved the probabilistic reliability assessment approach to account for different ductility observed in RTHS results. However, these studies focused on nonlinear structural behavior without degradation. Recent earthquake engineering research (Lignos and Krawinkler 2011, Hashemi and Mosqueda 2014) has brought attention to structural performance close to collapse which often experiences strength and stiffness degradation. In this study, nonlinear behavior of strength and stiffness degradation close to collapse is considered more extensively to validate the probabilistic approach for reliability assessment of RTHS results with the presence of actuator delay.

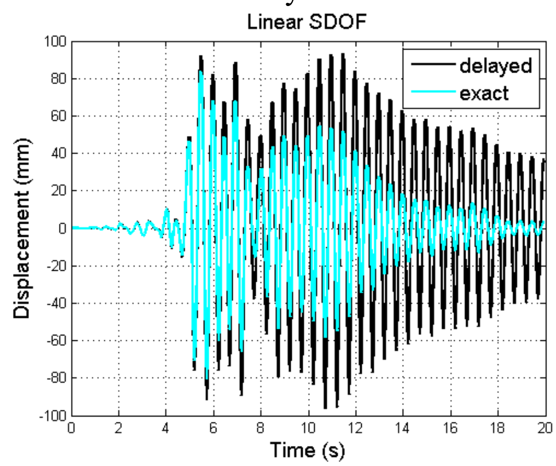

Figure 1. Comparison of structural responses for a linear SDOF Structure with 2 Hz natural frequency

2. GENERALIZED BOUC-WEN MODEL

In order to replicate the nonlinear behavior of structures near collapse, the generalized Bouc-Wen model is utilized in this study. During earthquakes, the response of the structure not only depends on the instantaneous deformation but also on the history of the deformation (Li *et al.* 2004). A mathematical model to describe this behavior was introduced by Bouc (1967) and Wen (1980). More recently, Baber and Wen (1981) and subsequently Baber and Noori (1985 and 1986) improved the model by incorporating strength and stiffness degradation and pinching respectively. This generalized Bouc-Wen model includes thirteen parameters as described in Table 1, which control the hysteresis shape. In this study, the generalized Bouc-Wen model is utilized to replicate the nonlinear behavior of structures near collapse. Figures 2(a) and 2(b) presents the hysteresis shape of a SDOF structure using the generalized Bouc-Wen model respectively.

Table1. Generalized Bouc-Wen model parameters

Parameter	Description	General Category
A	hysteretic shape controlling parameter	Basic Shape
β	hysteretic shape controlling parameter	
γ	hysteretic shape controlling parameter	
n	hysteretic shape controlling parameter	
α	ratio of post-yield stiffness to initial stiffness	
δη	Stiffness degradation controlling parameter	Degradation
δv	Strength degradation controlling parameter	
q	pinching initiation	Pinching
p	pinching slope	
ζs	a measuring total slip	
ψ	pinching magnitude	
δψ	pinching rate	
λ	pinching severity	

Using the generalized Bouc-Wen model, the equation of motion for a nonlinear SDOF can be described as following (Ma 2006):

$$m\ddot{x} + c\dot{x} + \alpha k x + (1-\alpha)kz = -m\ddot{x}_g \quad (1)$$

where *m* is the structural mass; *c* is the structural damping ration, α is the ratio of post yield stiffness to initial stiffness; *k* is the initial linear structural response; *x* is the structural displacement and (•) denotes a time derivative; $\ddot{x}_g$ is the ground acceleration; and z is the hysteresis displacement defined as following:

$$\dot{z} = h(z)\left\{\frac{A\dot{x}-(1+\delta_\nu\varepsilon)\left(\beta|\dot{x}||z|^{n-1}z+\gamma\dot{x}|z|^n\right)}{1+\delta_\eta\varepsilon}\right\} \quad (2)$$

where A, β, γ, and n are shape parameters; δ_ν and δ_η are strength and stiffness degradation parameters respectively; and ε is the dissipated hysteretic energy described by the equation:

$$\varepsilon = (1-\alpha)\omega_0^2\int_{t_0}^{t_f} z\,\dot{x}\,dt \quad (3)$$

The function $h(z)$ controls the pinching of the hysteresis and the hysteresis does not exhibit any pinching when $h(z) = 1$. $h(z)$ is calculated according to the equation below:

$$h(z) = 1-\zeta_s\left(1-e^{-p\varepsilon}\right)\cdot \exp\left(-\left(\frac{z\,\mathrm{sgn}(\dot{x})-\frac{q}{\left[(1+\delta_\nu\varepsilon)(\beta+\gamma)\right]^{\frac{1}{n}}}}{\left(\lambda+\zeta_s\left(1-e^{-p\varepsilon}\right)\right)\left(\psi+\delta_\psi\varepsilon\right)}\right)^2\right) \quad (4)$$

where $sgn(\bullet)$ denotes the signum function and ζ_s, p, q, λ, ψ, and δ_ψ are pinching parameters. The parameters for the generalized Bouc-Wen model used in this study are summarized in Table 2. Three different levels of stiffness and strength degradation (slight, moderate, and significant) along with the case of no degradation are examined and compared.

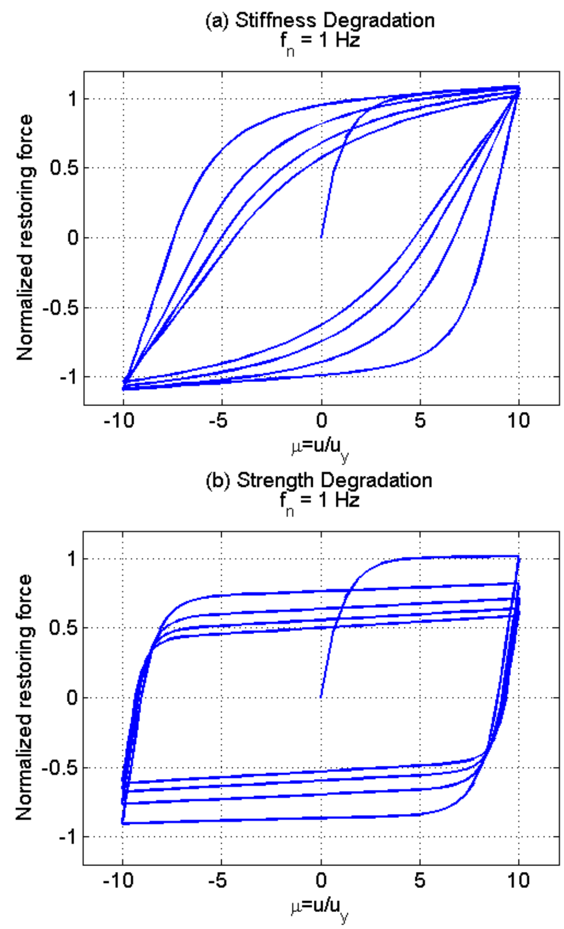

Figure 2. Hysteretic behavior using the generalized Bouc-Wen Model

Table 2. Bouc-Wen parameter values for analysis

Parameter	No Degradation	Stiffness Degradation			Strength Degradation		
		Slight	Moderate	Significant	Slight	Moderate	Significant
A	1	1	1	1	1	1	1
β	45	45	45	45	45	45	45
γ	55	55	55	55	55	55	55
n	2	2	2	2	2	2	2
α	0.01	0.01	0.01	0.01	0.01	0.01	0.01
δv	0	0	0	0	1	4	7
δη	0	2	6	9	0	0	0
p	0	0	0	0	0	0	0
q	0.15	0.15	0.15	0.15	0.15	0.15	0.15
ζs	0.9	0.9	0.9	0.9	0.9	0.9	0.9
ψ	0.1	0.1	0.1	0.1	0.1	0.1	0.1
δψ	0.005	0.005	0.005	0.005	0.005	0.005	0.005
λ	0.5	0.5	0.5	0.5	0.5	0.5	0.5

3. SIMULATION OF LINEAR-ELASTIC STRUCTURES

The effects of actuator delay on RTHS results of a linear elastic SDOF structure are first investigated. The prototype structure is assumed to have an inherent 2% viscous damping ratio. The equation of motion for such a SDOF can be derived from Eq. (1) as:

$$\ddot{x}(t) + c\dot{x}(t) + kx(t) = -\ddot{x}_g(t) \qquad (5a)$$

With the actuator delay existing in RTHS, the equation of motion can be modified as

$$\ddot{x}(t) + c\dot{x}(t) + kx(t-\tau) = -\ddot{x}_g(t) \qquad (5b)$$

where τ denotes the actuator delay.

A total of 44 far field records from FEMA P695 (2009) are used as ground motion inputs. These ground motions were selected by FEMA based on criteria such as source type, site conditions, and source magnitude. Names and magnitudes of these records are provided in Table 3.

Table 3.Far field ground motion records

ID No.	Earthquake			Recording Station	
	Year	M	Name	Name	Owenr
1	6.7	1994	Northridge	Beverly Hills-Mulhol	USC
2	6.7	1994	Northridge	Canyon County-WLC	USC
3	7.1	1999	Duze, Turkey	Bolu	ERD
4	7.1	1999	Hector Mine	Hector	SCSN
5	6.5	1979	Imperial Valley	Delta	UNAMUCSD
6	6.5	1979	Imperial Valley	El Centro Array #11	USGS
7	6.9	1995	Kobe, Japan	Nishi-Akashi	CUE
8	6.9	1995	Kobe, Japan	Shin-Osaka	CUE
9	7.5	1999	Kocaeli, Turkey	Duzce	ERD
10	7.5	1999	Kocaeli, Turkey	Arcelik	KOERI
11	7.3	1992	Landers	Yermo Fire Station	CDMG
12	7.3	1992	Landers	Cool Water	SCE
13	6.9	1989	Loma Prieta	Capitola	CDMG
14	6.9	1989	Loma Prieta	Gilroy Array #3	CDMG
15	7.4	1990	Manjil, Iran	Abbar	BHRC
16	6.5	1987	Superstition Hills	El Centro Imp. Co.	CDMG
17	6.5	1987	Superstition Hills	Poe Road Temp.	USGS
18	7.0	1992	Cape Mendocino	Rio Dell Over Pass	CDMG
19	7.6	1999	Chi-Chi Taiwan	CHY101	CWB
20	7.6	1999	Chi-Chi Taiwan	TCU045	CWB
21	6.6	1971	San Fernandino	LA - Hollywood Stor	CDMG
22	6.5	1976	Friuli, Italy	Tolmezzo	-

3.1 Accuracy Index

In order to analyze the simulation results, an accuracy index called MAX error was used, which is defined using the exact and the delayed displacement according to the equation below:

$$MAX = \frac{\max(|x_{ext} - x_{del}|)}{\max(|x_{ext}|)} \times 100\% \qquad (6)$$

where x_{ext} is the exact response from Eq. (5a); and x_{del} is the delayed response calculated from Eq. (5b). Chen *et al.* (2010) used a similar index for analyzing actuator control error when evaluating various compensation methods. It is also worth pointing that other formats of error such as root-mean-square is also used in this study but not presented herein due to limited length of paper.

3.2 Critical Delay Distribution

Critical delay is defined as the maximum delay that would lead to a MAX error close to a desired value. Critical delays corresponding to a target value of 10% are derived from computational simulation and then fit to a lognormal distribution using the maximum likelihood method (MLE).

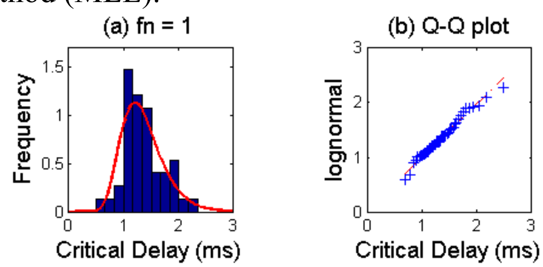

Figure 3. Histogram, fitted lognormal distribution, and Q-Q plot of the critical delay for a linear elastic SDOF structure with 1 Hz natural frequency.

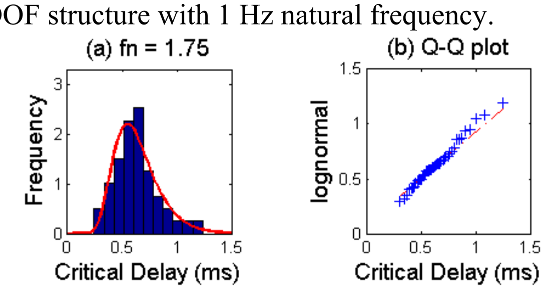

Figure 4. Histogram, fitted lognormal distribution, and Q-Q plot of the critical delay for a linear elastic SDOF structure with 1.75 Hz natural frequency.

Figures 3(a) and 4(a) present the histogram and the fitted lognormal distributions of critical delay for the linear elastic SDOF structure with 1.0 and 1.75 Hz natural frequency, respectively. Figures 3(b) and 4(b) present the quantile-quantile (Q-Q) plot as a goodness of fit for the lognormal distribution (Easton 1990). It can be observed that for the purposes of this study the proposed distribution is a good fit for the data.

3.3 Probabilistic Reliability Analysis

Chen and Rahul (2012) proposed the probabilistic reliability analysis based on the lognormal distribution in Figures 3(a) and 4(a). The probability that RTHS results have the error exceeding the target MAX error value is defined as the probability that the critical delay is smaller than the actual actuator delay in RTHS results. In this case the limit state function is written as given below:

$$g = \tau - d \tag{7}$$

where τ denotes the critical delay corresponding to the desired MAX error and d denotes the delay observed during RTHS. The probability of failure is thus the area under the distribution curve up to the delay τ as shown in Figure 5. It can be observed that the larger the actual delay in RTHS results, the higher the probability that the experimental results have MAX error exceeding the target value.

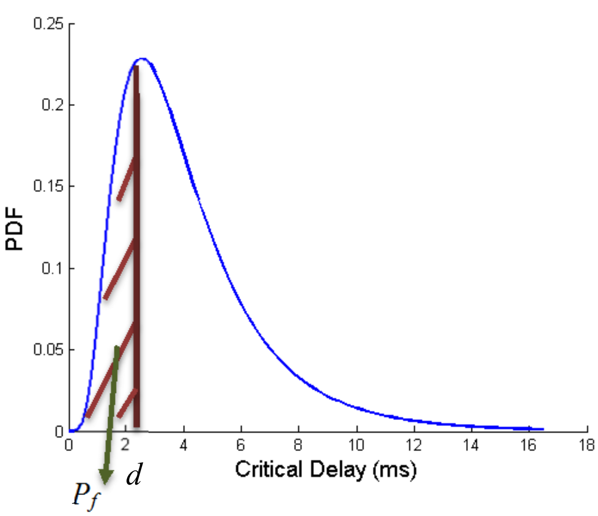

Figure 5. Probability of failure according to the PDF of Critical delay distribution.

4. NON-LINEAR SDOF WITH NO DEGRADATION

For the purpose of comparison, Bouc-Wen parameters are selected for no stiffness or strength degradation. Figure 6 presents MAX error corresponding to the ground motion recorded at the Canyon County-WLC station during the Northridge with peak ground acceleration (PGA) of 0.48g for five different natural frequencies. It can be observed that for a given value of delay, as the natural frequency increases, MAX error increases. Therefore, compensating for actuator error becomes even more critical when testing stiffer structures with higher natural frequencies.

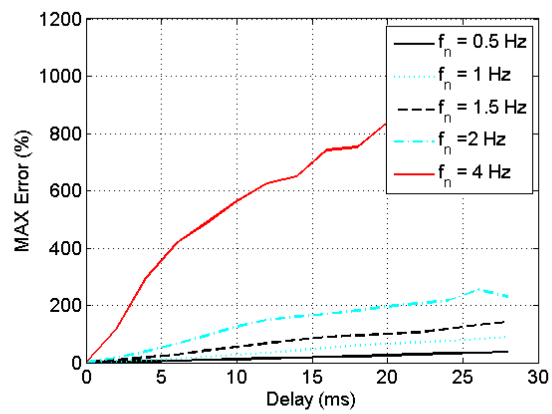

Figure 6. MAX error for different actuator delay.

5. NON-LINEAR SDOF WITH STIFFNESS AND STRENGTH DEGRADATION

Computational simulation is conducted for SDOF structure with stiffness and strength degradation. Figures 7(a), 8(a), and 9(a) present the histogram of the data along with the fitted lognormal distribution for a SDOF structure with slight, moderate and significant stiffness degradation, respectively. The SDOF structure has a natural frequency of 1 Hz. The lognormal distribution is observed to fit the data well. Figures 7(b), 8(b), 9(b) present the Q-Q plot for the corresponding cases. Slight deviation can be observed for the cases with moderate and significant stiffness degradation. Similar computational simulations are also conducted for SDOF structures with slight, moderate and significant strength degradation (Ryan 2014).

Figure 10(a) presents the probability density function of the lognormal distribution for SDOF structures with slight, moderate, and significant stiffness degradation data in comparison with the no degradation. The SDOF has a natural frequency of 1 Hz. It is observed that the mode of the distribution shifts to the left with increase in stiffness degradation. This implies that for the same delay, probability of inaccurate RTHS results increases with stiffness degradation. In other words, accurate actuator compensation is more critical when the experimental structure has significant stiffness degradation. Figure 10(b) presents the lognormal distribution corresponding to a SDOF structure with slight, moderate, and significant strength degradation in comparison with no degradation. It is observed that the lognormal distributions are identical with almost same values of mean and standard deviations. This implies that for reliability assessment, the probabilistic approach does not necessarily need to account for strength degradation.

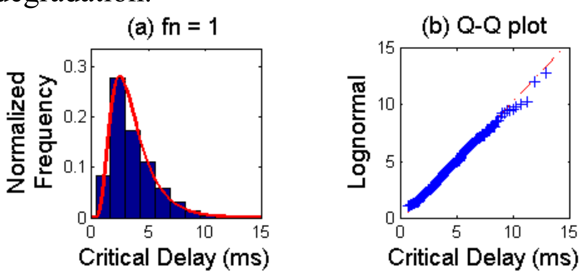

Figure 7. Histogram, Distribution, and Q-Q plot for a SDOF structure with slight stiffness degradation and a natural frequency of 1 Hz.

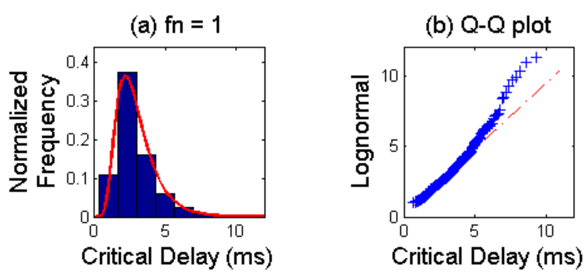

Figure 8. Histogram, Distribution, and Q-Q plot for a SDOF structure with moderate stiffness degradation and a natural frequency of 1 Hz.

Figure 11 presents the distribution of critical delay for SDOF structures with different natural frequencies and significant stiffness degradation. The critical delay is determined for 10% MAX error. It can be observed that, with the increase of natural frequency, distribution for critical delay has smaller values of mean and standard deviation.

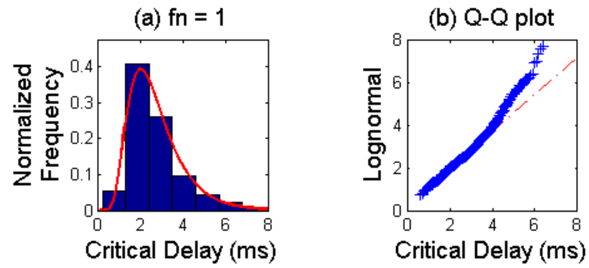

Figure 9. Histogram, Distribution, and Q-Q plot for a SDOF structure with significant stiffness degradation and a natural frequency of 1 Hz.

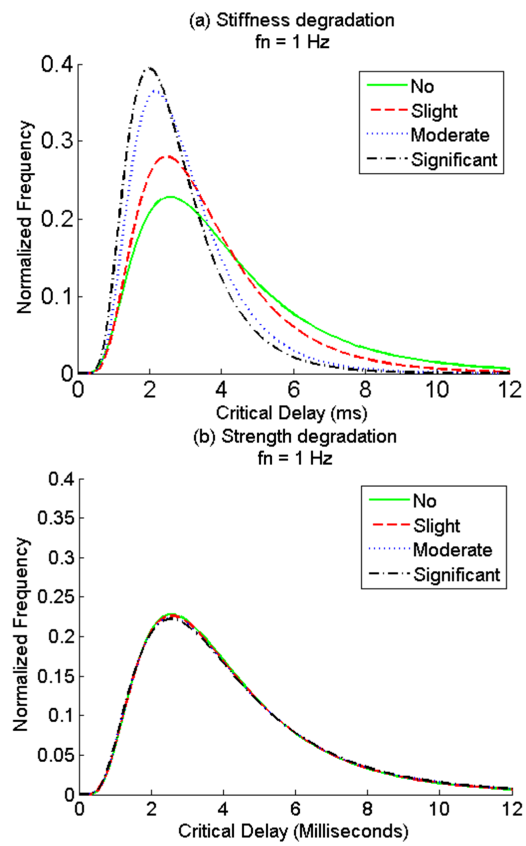

Figure 10. Comparison of critical delay distribution for different degradation cases for SDOF structure with natural frequency of 1 Hz.

6. DUCTILITY DEMAND AND CRITICAL DELAY

The relationship between ductility demand and critical delay is examined. For each critical delay data, the ductility demand is determined. Figure 13 presents the Critical delay distribution for different ductility demands for an SDOF with significant stiffness degradation. As the ductility demand increases, the distribution shifts to the right and becomes more dispersed.

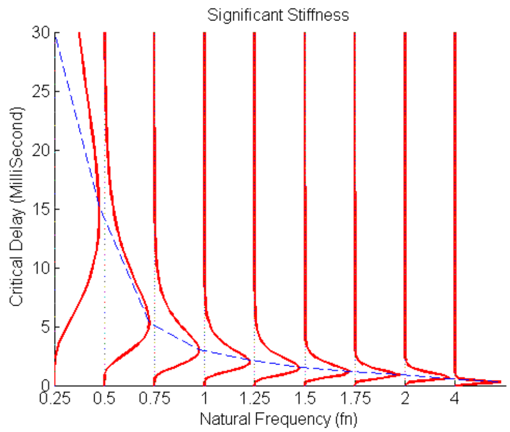

Figure 11. Distribution of critical delay for SDOF structures with different natural frequencies.

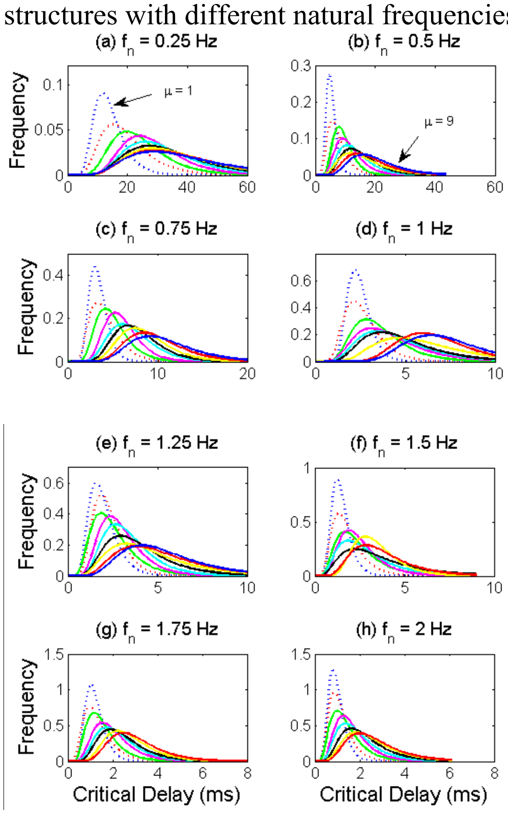

Figure 12. Critical delay distribution for different ductility demands for an SDOF with significant stiffness degradation.

7. EXAMPLES FOR PROBABILISTIC RELIABILITY ASSESSMENT

To illustrate reliability analysis using the proposed approach, a ground motion recorded during the Gazli USSR earthquake at the 9201 Karakyr station with a PGA of 0.69g is used for analysis at scales of 1, 2, 3 and 4. The SDOF structure is assumed to have a linear elastic natural frequency of 4 Hz, a damping ratio of 2%, with significant stiffness degradation. For the reliability analysis, the mean and the standard deviation of the critical delay distribution for ductility demand are determined from Figure 13. These distribution parameters are then used to find the probability that MAX Error is above 10% for the delay values. Table 4 presents the reliability analysis results compared with the MAX error values for each combination of scale and delay. The probabilistic method is observed to provide satisfactory results.

Table 4. Reliability Analysis Results

	Actuator Delay = 2 ms			
	Ground Motion Scale			
	1	2	3	4
Ductility Demand	1.111	2.620	4.751	8.430
Probability of Exceedance (%)	26.00	15.47	5.80	0.003
MAX Error (%)	5.94	4.08	5.42	2.41
	Actuator Delay = 4 ms			
	Ground Motion Scale			
	1	2	3	4
Ductility Demand	1.142	2.675	4.827	8.532
Probability of Exceedance (%)	97.0	74.80	46.27	4.15
MAX Error (%)	12.99	8.71	11.54	4.84
	Actuator Delay = 8 ms			
	Ground Motion Scale			
	1	2	3	4
Ductility Demand	1.209	2.785	5.035	8.712
Probability of Exceedance (%)	99.99	98.90	91.33	69.01
MAX Error (%)	30.69	18.92	23.78	9.63

8. SUMMARY AND CONCLUSION

A probabilistic approach for reliability analysis is further investigated for RTHS of structures with stiffness and strength degradation when actuator delay is present in servo-hydraulic actuator response. The generalized Bouc-Wen model is used in computation simulation to emulate nonlinear structural behavior with slight, moderate and significant stiffness and strength degradation. Lognormal distributions are established for critical delay corresponding to target error index considering different natural frequencies and different ductility demands. Stiffness degradation is observed to affect the critical delay and therefore need to be accounted for in reliability analysis, while critical delay distribution does not change based on strength degradation. Application of the probabilistic approach shows satisfactory results.

9. REFERENCES

Baber, T., and Wen, Y.K., (1981) "Random Vibration of Hysteretic Degrading Systems", Journal of Engineering Mechanics, ASCE, 107(EM6), 1069-10

Baber, T. Noori, M.N. (1985) "Random Vibration of Degrading Pinching Systems." Journal of Engineering Mechanics. 111, 1010:1026

Baber, T. Noori, M.N (1986) "Modeling General Hysteresis Behavior and Random Vibration Application." Journal of Vibration, Acoustics, Stress, and Reliability in Design. 108, 411-4200.

Bouc, R. (1967). "Forced Vibration of a Mechanical System with Hysteresis." Proc. 4th Conf. on nonlinear oscillations, Prague, Czechoslovakia

Chen, C., Ricles, J.M., Marullo, T. and Mercan, O. (2009). "Real-time hybrid testing using the unconditionally stable explicit CR integration algorithm." Earthquake Engineering and Structural Dynamics, 38(1), 23-44.

Chen, C., and Ricles, J.M., (2010). "Tracking Error-Based Servohydraulic Actuator Adaptive Compensation for Real-Time Hybrid Simulation." Journal of Structural Engineering, 135(4), 432-440

Chen, C., Ricles, J.M., Sause, R. and Christenson, R. (2010), "Experimental Evaluation of an Adaptive Actuator Control Technique for Real-Time Simulation of a Large-Scale Magneto-Rheological Fluid Damper," Smart Material and Structures, 19(2):025017.

Chen, C., Ricles, J. and Guo, T. (2012), "Improved Adaptive Inverse Compensation for Real-Time Hybrid Simulation," Journal of Engineering Mechanics, 138(12):1432-1446.

Chen, C. and Sharma, R. (2012), "A Reliability Assessment Approach for Real-Time Hybrid Simulation Results." Canadian Society for Civil Engineering annual conference and 3rd International Structural Specialty Conference, June 6-9, Edmonton, Alberta, Canada.

Chen, C., Valdovinos, J., and Santiallno, H. (2013), "Reliability Assessment of Real-Time Hybrid Simulation Results for Seismic Hazard Mitigation," Structures Congress 13, May 2- 4, Pittsburgh, PA.

Easton, G.S., McCulloch, R.E., (1990). "Multivariate Generalization of Quantile-Quantile Plots", Journal of the American Statistical Association, 85(410), 376-386

Federal Emergency Management Agency (2009). Quantification of building seismic performance factors, FEMA P-695. Washington, D.C.

Li, S.J., Suzuki, Y., and Noori, M. (2004), "Identification of hysteretic systems with slip using bootstrap filter." Mech Syst Signal Process 18, 781–795

Lignos, D.G., and Krawinkler, H. (2011). "Deterioration Modeling of Steel Beams and Columns in Support to Collapse Prediction of Steel Moment Frames," ASCE, Journal of Structural Engineering, 137 (11):1291-1302.

Ma, F., Ng, C.H., Ajavakom, N. (2006). "On system identification and response prediction of degrading structures." Structural Control and Health Monitoring, 13, 347-364.

Hashemi, M.J. and Mosqueda, G. (2014). "Innovative substructuring technique for hybrid simulation of multistory buildings through collapse," *Earthquake Engineering and Structural Dynamics*, 43(14): 2059–2074.

Ryan, H. (2014). Probabilistic Reliability Assessment of Real-Time Hybrid Simulation of Structures with Strength and Stiffness Degradation, master thesis, school of engineering, San Francisco State University.

Wen, Y.K. (1980). "Equivalent linearization for hysteretic systems under random excitation." Journal of Applied Mechanics, Transaction of ASME, 47, 150-154.